

# Homotopy Analysis solution for MHD flow and Heat Transfer of a Radiative Micropolar fluid over a Stretching Surface with Heat Generation/ Absorption

Kalpna Sharma, Sumit Gupta

Department of Mathematics, Swami Keshvanand Institute of Technology, Management and Gramothan, Jaipur-302017(INDIA)

*Email- guptasumit.edu@gmail.com*

Received 15.07.2018 received in revised form 31.08.2018, accepted 03.09.2018

**Abstract—** In this paper, (MHD) boundary layer flow and heat transfer of steady two dimensional flow of an electrically conducting micropolar fluid over a permeable stretching surface in presence of heat generation/absorption are discussed. By using similarity transformation, the arising governing equation of momentum and energy are transformed into coupled nonlinear ordinary differential equations, which are than solved by homotopy analysis method (HAM). The behavior of different physical parameters, namely, Prandtl number  $Pr$ , micro rotation parameter  $N$ , Magnetic parameter  $M$  and Radiation parameter  $R_d$  on the velocity and temperature profiles are depicted through graphically and tabular form in details. The present results are also compared with existing limiting solutions showing very good agreements with others.

**Keywords-** Micropolar fluid, MHD, Radiation, Heat Generation / Absorption, HAM.

## 1. INTRODUCTION

The fluid and heat transfer due a stretching sheet has been deliberate a remarkable applications such as industrialized of polymer sheet, filaments and wires, through the mechanized process. The stirring sheet is assumed to extend on its own plane and the protracted surface interacts with ambient fluid both impulsively and thermally. Sakiadas [1] first discuss the boundary layer flow over a surface. He discussed numerical solutions of laminar boundary-layer behavior on a moving continuous flat surface. Experimental and analytical behavior of this problem was presented by Tsou et al. [2] to show that such a flow is physically by validating Sakiadas [1] work. Crane [3] extended the work of Sakiadas [1] for both linearly and exponentially stretching sheet considering steady two-dimensional viscous flow. Free convective on a vertical stretching surface was discussed by Wang [4]. Heat transfer analysis over an exponentially stretching continuous surface with suction was presented by Elbashbeshy [5]. He obtained similarity solutions of the laminar boundary layer equations describing heat and flow in a quiescent fluid driven by an exponentially stretching surface with suction. Viscoelastic MHD flow heat and mass transfer over a stretching sheet with dissipation of energy and stress work was discussed by Khan

et al [6]. Ishak et al. [7] studied heat transfer over a stretching surface with variable heat flux in micropolar fluids. Nadeem et al. [8] coated boundary layer flow of a Jeffrey fluid over an exponential stretching surface with radiation effects. Recently Nadeem et al. [9] investigated the MHD boundary layer flow of a Casson fluid over an exponentially permeable stretching sheet.

The Homotopy analysis method (HAM) was first proposed by Shi Jun Liao [10] in 1992 to solve variety of nonlinear equations having various applications in science and engineering especially in fluid mechanics [11-12]. This technique does not depend upon the auxiliary parameter and converges very rapidly the approximate solution into exact one. Recently many researchers and scientists applied the HAM to various fluid flow problems with different geometries [13-17].

## 2. MATHEMATICAL FORMULATION

### 2.1. Mathematical formulation

Consider a two dimensional flow of an incompressible, electrically conducting incompressible micropolar fluid past a stretching surface. The sheet is coinciding with the plane  $y=0$  and origin is located at  $y=0$ , by which the sheet is stretching. A constant magnetic field of strength  $B_0$  is applied in a direction normal to the plane at  $y=0$ . The simplified two dimensional boundary layer equations governing the flow, and heat transfer are as follow:

$$\frac{\partial u}{\partial x} + \frac{\partial v}{\partial y} = 0 \quad (1)$$

$$u \frac{\partial u}{\partial x} + v \frac{\partial u}{\partial y} = \left( \frac{\mu + k}{\rho} \right) \frac{\partial^2 u}{\partial y^2} + \frac{k}{\rho} \frac{\partial N}{\partial y} - \frac{\sigma}{\rho} B_0^2 u, \quad (2)$$

$$G_1 \frac{\partial^2 N}{\partial y^2} - \left( 2N + \frac{\partial u}{\partial y} \right), \quad (3)$$

$$u \frac{\partial T}{\partial x} + v \frac{\partial T}{\partial y} = \frac{\kappa}{\rho c_p} \frac{\partial^2 T}{\partial y^2} + \frac{Q_0}{\rho c_p} (T - T_\infty) - \frac{1}{\rho c_p} \frac{\partial q_r}{\partial y}, \quad (4)$$

The associate boundary conditions are

$$u = U_w(x) = ax, \quad v = V_w, \quad N = 0, \quad \frac{\partial T}{\partial y} = -\frac{bx^m}{\kappa} \quad \text{at } y = 0,$$

$$u_y \rightarrow 0, \quad u \rightarrow 0, \quad N \rightarrow 0, \quad T \rightarrow T_\infty \quad \text{at } y \rightarrow \infty, \quad (5)$$

where  $u$  and  $v$  are the velocity components in  $x$  and  $y$  direction, respectively.  $a > 0$  is known as stretching rate,  $\nu$  is the kinematic viscosity,  $N$  is the micro-rotation parameter,

$G_1 = \frac{\gamma}{k}$  is the micro-rotation constant,  $\rho$  is the density of base fluid,  $\sigma$  is the electrical conductivity, and  $T$  is the ambient fluid temperature,  $Q_0$  is the internal heat generation/absorption coefficient,  $c_p$  is the specific heat at constant pressure. Here  $T_w$  and  $T_\infty$  are the temperature of the fluid at the wall and ambient temperature

Using Rosseland approximation for radiation, we have

$$q_r = -\frac{4\sigma^* \partial T^4}{3k^* \partial y} \quad (6)$$

where  $\sigma^*$  is the Stefan-Boltzman constant, and  $k^*$  is the mean absorption coefficient. Expanding  $T^4$  in terms of Taylor series about  $T_\infty$  (the free stream temperature) and neglecting higher order terms, we have  $T^4 \approx 4T_\infty^3 T - 3T_\infty^4$ . (7)

using (6) in (7) we get

$$\frac{\partial q_r}{\partial y} = -\frac{16\sigma^* T_\infty^3}{3k^*} \frac{\partial^2 T}{\partial y^2} \quad (8)$$

Introducing the following similarity transformation

$$\psi = \sqrt{av} f(\eta), \theta(\eta) = \frac{T - T_\infty}{T_w - T_\infty}, N = ax\sqrt{\frac{a}{\nu}} h(\eta), \eta = \sqrt{\frac{a}{\nu}} y \quad (9)$$

Where the stream function  $\psi$  is defined as

$$u = \frac{\partial \psi}{\partial y} \quad \text{and} \quad v = -\frac{\partial \psi}{\partial x} \quad (10)$$

using equations (9)-(10) in equations (1)-(4), the equations of linear momentum and energy with their corresponding boundary conditions are as follows

$$(1 + K)f'''' + f f'' - f'^2 - M f' + K h' = 0, \quad (11)$$

$$\left(1 + \frac{4}{3} R_d\right) \theta'' + \text{Pr} (f \theta' - m f' \theta + \tau \theta) = 0. \quad (12)$$

$$Gh'' - (2h + f'') = 0 \quad (13)$$

Subject to the boundary conditions are as follows

$$f = f_w, f' = 1, h = 0, \theta' = -1 \text{ at } \eta = 0$$

$$f \rightarrow 0, h \rightarrow 0, \theta \rightarrow 0 \text{ at } \eta \rightarrow \infty \quad (14)$$

Where  $M = \sqrt{\frac{\sigma}{c\rho_f}} B_0$  is the dimensionless magnetic parameter,  $\text{Pr} = \frac{\nu}{\alpha}$  is the Prandtl number,  $K = \frac{k}{\mu}$  is the

material parameter,  $G = \frac{G_1 a}{\nu}$  is the micro-rotation parameter,

$\tau = \frac{Q_0}{a\rho c_p}$  is the heat generation ( $> 0$ ) or absorption ( $< 0$ )

parameter and  $f_w = -\frac{v_w}{\sqrt{av}}$  is the suction ( $> 0$ ) or injection parameter ( $< 0$ ).

The skin friction coefficient and the local Nusselt numbers are defines as

$$C_f = \frac{\tau_w}{\rho_f u_w^2(x)}, \quad Nu_x = \frac{xq_w}{k(T_w - T_\infty)} \quad (15)$$

Where  $\tau_w$  is the shear stress along the stretching surface and  $q_w$  is the surface heat flux, are given by

$$\tau_w = \mu \left( \frac{\partial u}{\partial y} \right)_{y=0}, \quad q_w = -\alpha \left( \frac{\partial T}{\partial y} \right)_{y=0} \quad (16)$$

Using the non-dimensional variables we obtain

$$\sqrt{\text{Re}_x} C_f = f''(0), \quad \frac{Nu_x}{\sqrt{\text{Re}_x}} = \left(1 + \frac{4R_d}{3}\right) \theta'(0) \quad (17)$$

Where  $\text{Re}_x = \frac{xu_w(x)}{\nu}$  is the local Reynolds's number

### Solution of the Problem by the homotopy analysis method

The dimensionless velocities  $f(\eta), h(\eta)$  and the temperature  $\theta(\eta)$  can be expressed by the set of base functions.

$$\{\eta^k \exp(-n\eta) | k \geq 0, n \geq 0\},$$

By rule of solution expressions and the boundary conditions (14), the initial guesses  $f_0, h_0$  and  $\theta_0$  are selected as

$$f_0(\eta) = f_w + 1 - \exp(-\eta), \quad (18)$$

$$h_0(\eta) = 1 - \exp(-\eta) \quad (19)$$

$$\theta_0(\eta) = \exp(-\eta). \quad Gh'' - (2h + f'') = 0, \quad (20)$$

with the linear operators as

$$L_f = \frac{d^3 f}{d\eta^3} - \frac{df}{d\eta}, \quad (21)$$

$$L_h = \frac{d^2 h}{d\eta^2} - h, \quad (22)$$

$$L_\theta = \frac{d^2 \theta}{d\eta^2} - \theta, \quad (23)$$

with the property that

$$L_f [C_1 + C_2 \exp(-\eta) + C_3 \exp(\eta)] = 0, \quad (24)$$

$$L_h [C_4 \exp(-\eta) + C_5 \exp(\eta)] = 0, \quad (25)$$

$$L_\theta [C_6 \exp(-\eta) + C_7 \exp(\eta)] = 0. \tag{26}$$

where  $C_i, i = 1..7$  are arbitrary constants

The zeroth order deformation problems can be written as

$$(1-p)L_f[\hat{f}(\eta; p) - f_0(\eta)] = p\hbar_f N_f[\hat{f}(\eta; p), \hat{h}(\eta; p), \hat{\theta}(\eta; p)], \tag{27}$$

$$(1-p)L_h[\hat{h}(\eta; p) - h_0(\eta)] = p\hbar_h N_h[\hat{h}(\eta; p), \hat{f}(\eta; p), \hat{\theta}(\eta; p)], \tag{28}$$

$$(1-p)L_\theta[\hat{\theta}(\eta; p) - \theta_0(\eta)] = p\hbar_\theta N_\theta[\hat{f}(\eta; p), \hat{h}(\eta; p), \hat{\theta}(\eta; p)]. \tag{29}$$

where  $p \in [0, 1]$  indicates the embedding parameter and  $\hbar_f, \hbar_h$  and  $\hbar_\theta$  the nonzero auxiliary parameters. Moreover the nonlinear operators  $N_f, N_h$  and  $N_\theta$  are prescribed as

$$N_f[\hat{f}(\eta; p), \hat{h}(\eta; p), \hat{\theta}(\eta; p)] = \frac{\partial^3 \hat{f}(\eta; p)}{\partial \eta^3} + \hat{f}(\eta; p) \frac{\partial^2 \hat{f}(\eta; p)}{\partial \eta^2} - \left( \frac{\partial \hat{f}(\eta; p)}{\partial \eta} \right)^2 + K \frac{\partial \hat{h}(\eta; p)}{\partial \eta} - M \frac{\partial \hat{f}(\eta; p)}{\partial \eta}, \tag{30}$$

$$N_h[\hat{f}(\eta; p), \hat{h}(\eta; p), \hat{\theta}(\eta; p)] = G \frac{\partial^2 \hat{h}(\eta; p)}{\partial \eta^2} - \left( 2\hat{h}(\eta; p) + \frac{\partial^2 \hat{f}(\eta; p)}{\partial \eta^2} \right) \tag{31}$$

$$N_\theta[\hat{f}(\eta; p), \hat{\theta}(\eta; p)] = \left( 1 + \frac{4}{3} R_d \right) \frac{\partial^2 \hat{\theta}(\eta; p)}{\partial \eta^2} + \Pr \left( \hat{f}(\eta; p) \frac{\partial \hat{\theta}(\eta; p)}{\partial \eta} - m \frac{\partial \hat{f}(\eta; p)}{\partial \eta} \hat{\theta}(\eta; p) + \tau \hat{\theta}(\eta; p) \right) \tag{32}$$

For  $p = 0$  and  $p = 1$  we have

$$\hat{f}(\eta; 0) = f_0(\eta), \quad \hat{f}(\eta; 1) = f(\eta), \tag{33}$$

$$\hat{h}(\eta; 0) = h_0(\eta), \quad \hat{h}(\eta; 1) = h(\eta), \tag{34}$$

$$\hat{\theta}(\eta; 0) = \theta_0(\eta), \quad \hat{\theta}(\eta; 1) = \theta(\eta). \tag{35}$$

By means of Taylor's series we have

$$\hat{f}(\eta; p) = f_0(\eta) + \sum_{m=1}^{\infty} f_m(\eta) p^m, \tag{36}$$

$$\hat{h}(\eta; p) = h_0(\eta) + \sum_{m=1}^{\infty} h_m(\eta) p^m, \tag{37}$$

$$\hat{\theta}(\eta; p) = \theta_0(\eta) + \sum_{m=1}^{\infty} \theta_m(\eta) p^m. \tag{38}$$

$$f_m(\eta) = \frac{1}{m!} \left( \frac{\partial^m f(\eta; p)}{\partial \eta^m} \right)_{p=0}, \quad h_m(\eta) = \frac{1}{m!} \left( \frac{\partial^m h(\eta; p)}{\partial \eta^m} \right)_{p=0}, \quad \theta_m(\eta) = \frac{1}{m!} \left( \frac{\partial^m \theta(\eta; p)}{\partial \eta^m} \right)_{p=0}. \tag{39}$$

auxiliary parameters are so properly chosen that series (31)-(32) converges when  $p=1$  and thus

$$f(\eta) = f_0(\eta) + \sum_{m=1}^{\infty} f_m(\eta), \tag{40}$$

$$h(\eta) = h_0(\eta) + \sum_{m=1}^{\infty} h_m(\eta), \tag{41}$$

$$\theta(\eta) = \theta_0(\eta) + \sum_{m=1}^{\infty} \theta_m(\eta). \tag{42}$$

The resulting problems at the  $m$ th-order deformation are

$$L_f[f_m(\eta) - \chi_m f_{m-1}(\eta)] = \hbar_f \mathfrak{R}_m^f(\eta), \tag{43}$$

$$L_h[h_m(\eta) - \chi_m h_{m-1}(\eta)] = \hbar_h \mathfrak{R}_m^h(\eta), \tag{44}$$

$$L_\theta[\theta_m(\eta) - \chi_m \theta_{m-1}(\eta)] = \hbar_\theta \mathfrak{R}_m^\theta(\eta), \tag{45}$$

$$\text{in which } \chi_m = \begin{cases} 0, & m \leq 1, \\ 1, & m > 1, \end{cases}$$

$$\text{and } \mathfrak{R}_m^f(\eta) = (1+K)f_{m-1}'' + \sum_{k=0}^{m-1} (f_k f_{m-1-k}'' - f_k' f_{m-1-k}' + K h_{m-1}' - M f_{m-1}') \tag{46}$$

$$\mathfrak{R}_m^h(\eta) = G h_{m-1}'' - (2 h_{m-1} + f_{m-1}'') \tag{47}$$

$$\mathfrak{R}_m^\theta(\eta) = \theta_{m-1}'' + \Pr \sum_{k=0}^{m-1} (f_k \theta_{m-1-k}' - f_k' \theta_{m-1-k}') + \Pr \tau \theta_{m-1} \tag{48}$$

The general solutions of Eqs. (11)-(13) can be written as

$$f_m(\eta) = f_m^*(\eta) + C_1 + C_2 \exp(-\eta) + C_3 \exp(\eta), \tag{49}$$

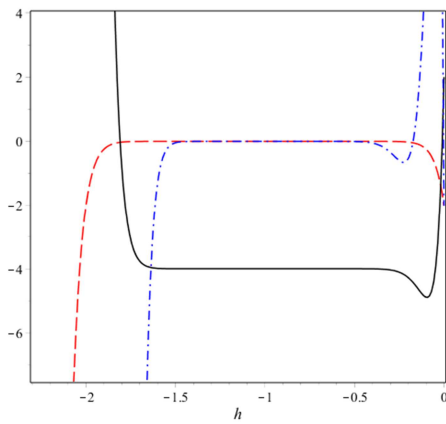
$$h_m(\eta) = h_m^*(\eta) + C_4 \exp(-\eta) + C_5 \exp(\eta), \tag{50}$$

$$\theta_m(\eta) = \theta_m^*(\eta) + C_6 \exp(-\eta) + C_7 \exp(\eta). \tag{51}$$

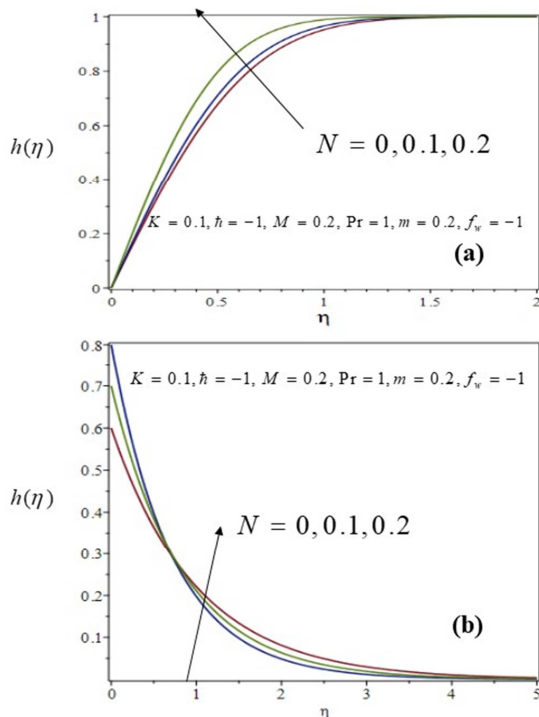
in which  $f_m^*(\eta), h_m^*(\eta)$  and  $\theta_m^*(\eta)$  are the particular solutions of the Eqs. (43)- (45). Note that the Eqs. (42)- (43) can be solved by Mathematica, Maple and Matlab one after the other in the order  $m = 1, 2, 3, \dots$

### 3. GRAPHICS PREPARATION

It can be noticed that the series solutions (43)-(45) contain the non-zero auxiliary parameters  $\hbar_f, \hbar_h$  and  $\hbar_\theta$ . We can adjust and control the convergence of the HAM solutions with the help of these auxiliary parameters. Hence to compute the range of admissible values of  $\hbar_f, \hbar_h$  and  $\hbar_\theta$ , we display the  $\hbar$ -curve of the functions  $f''(0), h'(0)$  and  $\theta'(0)$  of 15<sup>th</sup>-order of approximations. Fig.1 depicts that the range of admissible values of  $\hbar_f, \hbar_h$  and  $\hbar_\theta$  are  $-1.8 \leq \hbar_f \leq -0.15, -1.5 \leq \hbar_h \leq -0.5$  and  $-1.7 \leq \hbar_\theta \leq -0.3$ . The series solution (43)-(45) converge in the whole region of  $\eta$  when  $\hbar_f = \hbar_h = \hbar_\theta = -1.12$ . In this paper, the variations of emerging parameters on the fluid flow and heat transfer rate are being discussed and to show physical behavior of the flow problems, the velocity, temperature and heat transfer are plotted in Figs [2-4].

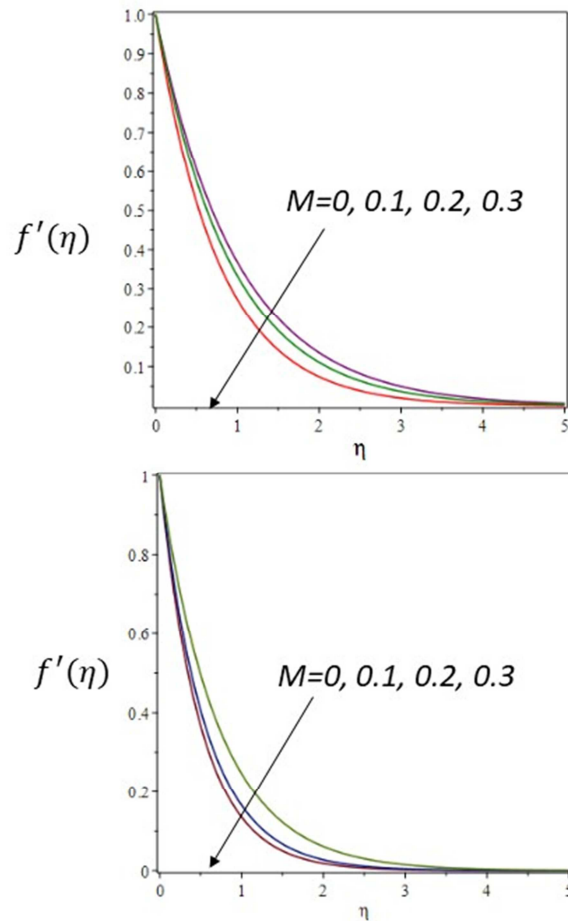


**Figure 1 :**  $\hat{h}$  curve for 15<sup>th</sup> order approximations for red dashed line, blue dot-dashed line and solid line of  $f''(0)$ ,  $h'(0)$  and  $\theta'(0)$  respectively



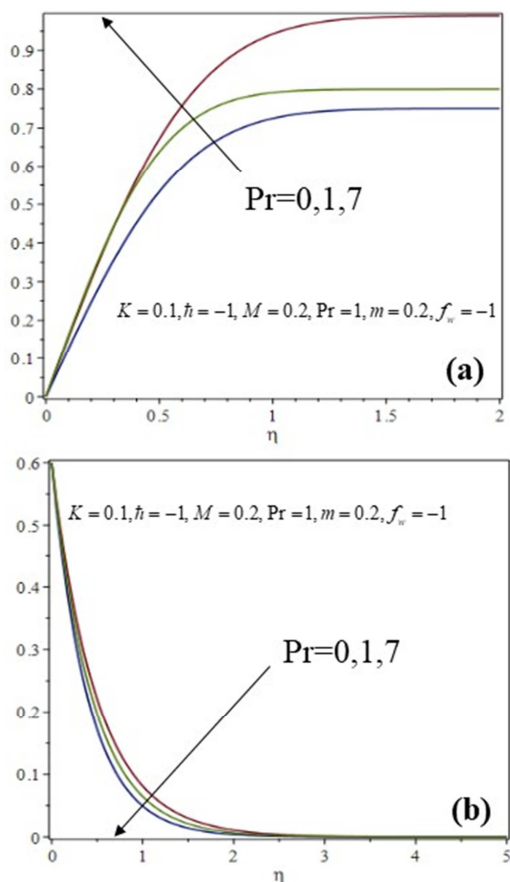
**Figure3 :** Transverse velocity profile versus Rotation parameter in the case of suction (a) and injection (b)

Fig 2 (a) and (b) shows the effects of the magnetic field parameter  $M$  on the velocity profile. It is observe that with increase of magnetic parameter  $M$  the velocity is decreases. This is the fact that in presence of magnetic field, a Lorentz force acts against the fluid flow, which retards the velocity of the fluid within the boundary layer thickness for both suction and injection. Fig 3 (a) and (b) shows the effects of the rotational motion parameter  $N$  on the transverse velocity. It is observe that with increase of rotational motion parameter the velocity is increases. This is due to fact that the more rotation in rpm requires more power to rotating the fluid within the boundary layer thickness, so the velocity is also increases for both suction and injection.



**Figure 2 :** Velocity profile versus magnetic parameter in the case of suction (a) (top) and injection (b) (bottom)

Fig. 4 (a) and (b) represented the effect of Prandtl number on the temperature profiles in the boundary layer for stretching surface. It has been noticed that the temperature decreases with the increase of the Prandtl number. This is the fact that the increases in the Prandtl number decrease the thermal boundary layer thickness, lower the temperature within the boundary layer with increases the Prandtl number. Prandtl number shows the ratio of momentum diffusivity to thermal diffusivity. The figure reveals that an increase in Prandtl number  $Pr$ , results in a decrease in the temperature distribution at a particular point of flow.



**Figure 4 :** Temperature profile versus Prandtl number in the case of suction (a) and injection (b)

#### 4. CONCLUSION

The series solution of (MHD) boundary layer flow and heat transfer of steady two dimensional flow of an electrically conducting micropolar fluid over a permeable stretching surface in presence of heat generation/ absorption is discussed. The behavior of embedding parameter is examined. An analytical technique well known as homotopy analysis method (HAM) has been applied to determine the solutions of the governing non-linear ordinary differential equations. Graphical illustrations were shown subsequent to the flow characteristics for the velocity and temperature with the various associated physical parameters.

#### REFERENCES

- [1] B. C. Sakiadas, Boundary layer behavior on continuous solid flat surfaces, *J.A.I.Ch.E.J* 7 (1961) 26-28.
- [2] F. K. Tsou, E. M. Sparrow, R. J. Goldstein, Flow and heat transfer in the boundary layer on a continuous moving surface, *Int.J Heat Mass Transfer* 10 (1967) 219-235.
- [3] L. Crane, Flow past a stretching plate, *ZAMP* 21 (1970) 645-647.
- [4] C. Y. Wang, Free convection on a vertical stretching surface, *J. App Math Mech (ZAMM)*, 69 (1989) 418-420.
- [5] E. M. A. Elbashaeshy, Heat transfer over an exponentially stretching continuous surface with suction, *Arch. Mech* 53 (2001) 643-651.

- [6] S. K. Khan, M. S. Abel, R. M. Sonth, Viscoelastic MHD flow Heat and Mass transfer over a stretching sheet with dissipation of energy and stress work, *Heat Mass Trans.* 40 (2004) 7-57.
- [7] A. Ishak, R. Nazar, I. Pop, Heat transfer over a stretching surface with variable heat flux in micropolar fluids, *Phys. Lett. A.* 372 (2008) 559-561.
- [8] S. Nadeem, S. Zaheer, T. Fang, Effects of thermal radiation on the boundary layer flow of a Jeffrey fluid over an exponentially stretching surface. *Numer Algo.* 57 (2011) 187-205.
- [9] S. Nadeem, R. Haq, C. Lee, MHD flow of a Casson fluid over an exponentially stretching sheet, *Scien. Iran. B* 19 (2012) 1550-1553.
- [10] S. J. Liao, Homotopy analysis method in nonlinear differential equation, Springer, Heidelberg, Germany, 2012.
- [11] S. J. Liao, An optimal homotopy analysis approach for strongly nonlinear differential equations, *Commun. Non Linear Sci. Numer. Simul.* 15, 2010, 2003-2016.
- [12] S. J. Liao, Advances in the homotopy analysis method, World Scientific, ISBN 978-9814551243, 2013.
- [13] S. Gupta, K. Sharma, Numerical simulation for magnetohydrodynamic three dimensional flow of Casson nanofluid with convective boundary conditions and thermal radiation, *Engineering Computations*, 34 (8), 2017, 2698-2722.
- [14] S. Gupta, D. Kumar, J. Singh, MHD mixed convective stagnation point flow and heat transfer of an incompressible nanofluid over an inclined stretching sheet with chemical reaction and radiation, *International Journal of Heat and Mass Transfer*, 118, 2018, 378-387.
- [15] K. Sharma, S. Gupta, Viscous dissipation and thermal radiation effects in MHD flow of Jeffrey nanofluid through impermeable surface with heat generation/absorption, *Nonlinear Engineering*, 6 (2), 2017, 153-166.
- [16] K. Sharma, S. Gupta, Homotopy analysis solution to thermal radiation effects on MHD boundary layer flow and heat transfer towards an inclined plate with convective boundary conditions, *International Journal of Applied and Computational Mathematics*, 3 (3), 2017, 2533-2552.
- [17] S. Gupta, K. Sharma, Mixed Convective MHD Flow and Heat Transfer of Uniformly Conducting Nanofluid Past an Inclined Cylinder in Presence of Thermal Radiation, *Journal of nanofluids*, 6 (6), 2017, 1031-1045.